Available online at www.sciencedirect.com
ScienceDirect
Geochimica et Cosmochimica Acta 72 (2008) 345–359
Geochimica et Cosmochimica Acta
www.elsevier.com/locate/gca

Natural fractionation of $^{238}U/^{235}U$

S. Weyer [a,*], A.D. Anbar [b], A. Gerdes [a], G.W. Gordon [b], T.J. Algeo [c], E.A. Boyle [d]

[a] University of Frankfurt, Institute of Geosciences, Altenhofer Allee 1, D-60431 Frankfurt, Germany
[b] Arizona State University, School of Earth & Space Exploration, Tempe, AZ 85287, USA
[c] University of Cincinnati, Department of Geology, 500 Geology/Physics Bldg., Cincinnati, OH 45221-0013, USA
[d] Massachusetts Institute of Technology, Earth, Atmospheric and Planetary Sciences, 77 Massachusetts Avenue, Cambridge MA 02139, USA

Received 23 July 2007; accepted in revised form 9 November 2007; available online 22 November 2007

Abstract

The isotopic composition of U in nature is generally assumed to be invariant. Here, we report variations of the $^{238}U/^{235}U$ isotope ratio in natural samples (basalts, granites, seawater, corals, black shales, suboxic sediments, ferromanganese crusts/nodules and BIFs) of ~1.3‰, exceeding by far the analytical precision of our method (≈0.06‰, 2SD). U isotopes were analyzed with MC-ICP-MS using a mixed ^{236}U–^{233}U isotopic tracer (double spike) to correct for isotope fractionation during sample purification and instrumental mass bias. The largest isotope variations found in our survey are between oxidized and reduced depositional environments, with seawater and suboxic sediments falling in between. Light U isotope compositions (relative to SRM-950a) were observed for manganese crusts from the Atlantic and Pacific oceans, which display $\delta^{238}U$ of −0.54‰ to −0.62‰ and for three of four analyzed Banded Iron Formations, which have $\delta^{238}U$ of −0.89‰, −0.72‰ and −0.70‰, respectively. High $\delta^{238}U$ values are observed for black shales from the Black Sea (unit-I and unit-II) and three Kupferschiefer samples (Germany), which display $\delta^{238}U$ of −0.06‰ to +0.43‰. Also, suboxic sediments have slightly elevated $\delta^{238}U$ (−0.41‰ to −0.16‰) compared to seawater, which has $\delta^{238}U$ of -0.41 ± 0.03‰. Granites define a range of $\delta^{238}U$ between −0.20‰ and −0.46‰, but all analyzed basalts are identical within uncertainties and slightly lighter than seawater ($\delta^{238}U = -0.29$‰).

Our findings imply that U isotope fractionation occurs in both oxic (manganese crusts) and suboxic to euxinic environments with opposite directions. In the first case, we hypothesize that this fractionation results from adsorption of U to ferromanganese oxides, as is the case for Mo and possibly Tl isotopes. In the second case, reduction of soluble U^{VI} to insoluble U^{IV} probably results in fractionation toward heavy U isotope compositions relative to seawater. These findings imply that variable ocean redox conditions through geological time should result in variations of the seawater U isotope compositions, which may be recorded in sediments or fossils. Thus, U isotopes might be a promising novel geochemical tracer for paleo-redox conditions and the redox evolution on Earth. The discovery that $^{238}U/^{235}U$ varies in nature also has implications for the precision and accuracy of U–Pb dating. The total observed range in U isotope compositions would produce variations in $^{207}Pb/^{206}Pb$ ages of young U-bearing minerals of up to 3 Ma, and up to 2 Ma for minerals that are 3 billion years old.

1. INTRODUCTION

During the last decade, transition metals and other heavy elements have joined the lighter elements as targets for intensive stable isotope investigation. This development followed from the invention and refinement of multiple collector ICP-MS (MC-ICP-MS) techniques (Walder and Freedman, 1992; Halliday et al., 1998; Maréchal et al., 1999; Weyer and Schwieters, 2003) that enable measurements of non-radiogenic variations in the isotope compositions of such elements to a precision on the order of 0.1‰ (or better). As a result, it is now practical to study stable isotope variations across the periodic table, e.g., Cr, Fe, Cu, Zn, Mo, Cd and Tl (e.g., Rehkämper et al., 2002;

* Corresponding author. Fax: +49 69 798 40121.
E-mail address: stefan.weyer@em.uni-frankfurt.de (S. Weyer).

0016-7037/$ - see front matter © 2007 Elsevier Ltd. All rights reserved.
doi:10.1016/j.gca.2007.11.012

Wombacher et al., 2003; Albarede, 2004; Anbar, 2004; Johnson et al., 2004; Johnson and Bullen, 2004). Although relative mass differences are rather small, surprisingly large (per-mil level) isotope variations, are observed even for very heavy elements, such as Hg and Tl (e.g., Rehkämper et al., 2002; Bergquist and Blum, 2007). Significant equilibrium isotope fractionation for these elements is possible because of the ''nuclear field shift'' effect (Bigeleisen, 1996; Schauble, 2007), a fractionation mechanism related to nuclear volume rather than to mass that operates independently of traditional, vibrationally-derived, mass-dependent fractionation. According to the modeling of Schauble (2006), this volume effect should also produce significant U isotope fractionation on the ‰ level at typical environmental temperatures (≈25 °C). Here, we investigate natural variations in the isotope composition of the heaviest naturally-occurring element—uranium.

Uranium has five isotopes with a half-life of longer than 10^5 years. Two of these isotopes, ^{238}U and ^{235}U, are primordial, with half-lives of 4.468×10^9 yr and 0.7038×10^9 yr, respectively. Their respective natural abundances, 99.28% and 0.72%, are high enough for precise isotope measurements with MC-ICP-MS. However, none of the U isotopes is stable. Thus, the term ''stable isotope fractionation'' cannot be used for U, although mechanisms leading to isotope variations in natural samples may be the same as for other heavy stable isotopes. Although the $^{238}U/^{235}U$ isotope ratio has changed dramatically during Earth history from about 3.3 to the present-day value of 137.88 (Cowan and Adler, 1976; Rosman and Taylor, 1998), the natural variations we observed on Earth today must have been produced by chemical reactions that fractionate isotopes. Natural variations due to radioactive decay are only possible in the oldest fragments of meteorites that may preserve U isotope variations resulting from the decay of ^{247}Cm to ^{235}U (Stirling et al., 2005). Another isotope, ^{234}U also occurs in nature as a decay product of ^{238}U (with an abundance of ≈0.0054% and a half-life of 2.48×10^5 yr). Large natural variations (>10%) are seen in $^{234}U/^{238}U$ due to the effect of alpha recoil on the relative rates of release of these isotopes from minerals (Kronberg, 1974; Henderson et al., 2001). The remaining two U isotopes, ^{233}U and ^{236}U, have half-lives of 1.59×10^5 yr and 2.34×10^7 yr, respectively, and so basically do not occur in nature.

Significant isotope fractionation effects could be expressed in association with a variety of chemical transformations, particularly during low-temperature processes. These may include adsorption, changes in U speciation, or redox chemistry (including microbially-mediated reduction). Redox chemistry could be particularly important because U commonly occurs in two redox states in nature, U^{IV} and U^{VI}. It is very soluble in oxygenated water because the predominant uranyl ion $U^{VI}O_2^{2-}$ is stabilized by the formation of soluble and non-reactive carbonate complexes (Langmuir, 1978; Klinkhammer and Palmer, 1991; Calvert and Pedersen, 1993). Consequently, U has a long ocean residence time in modern seawater (≈0.5 Ma; Ku et al., 1977; Cochran et al., 1986; Dunk et al., 2002). Reduction to U^{IV} is probably important for U removal from the oceans in suboxic and anoxic environments (Anderson, 1987; Barnes and Cochran, 1990; Klinkhammer and Palmer, 1991; Morford and Emerson, 1999; McManus et al., 2006). Microorganisms probably have a large impact on U mobility and might generally play an essential role for U reduction, including the formation of U deposits (Barnes and Cochran, 1990; Klinkhammer and Palmer, 1991; Lovely et al., 1991; Lovley, 1993; Wersin et al., 1994; Suzuki and Banfield, 1999; Zheng et al., 2002b). Therefore, significant U isotope fractionation should be possible at the Earth's surface and may thus be a useful tool in life-, ocean- or environmental sciences. Indeed, U isotope fractionation has been observed very recently during bacterial U-reduction experiments (using the SRM U-500 standard (Rademacher et al., 2006) and in natural environments (Stirling et al., in press)). Notably, U isotope fractionation, might also affect the precision of high-precision U–Th–Pb geochronology (Stirling et al., in press). Our study was motivated by these considerations.

2. ANALYTICAL TECHNIQUES

2.1. Sample digestions

All solid samples were powdered and precisely weighted before digestion. For granites about 20–50 mg and for basalts up to 300 mg were digested with a mixture of conc. HF/HNO_3 (3:1) in 15 ml Savilex® beakers (basalts on a hot plate at 120 °C and granites in Parr® high-pressure vessels at 180 °C). Afterwards, samples were repeatedly treated with 6 M HNO_3 and 6 M HCl to dissolve any remaining fluorites. For organic-rich sediments, such as black shales and suboxic margin sediments, about 20–100 mg was ashed in ceramic vessels at 550 °C overnight. The residue was quantitatively transferred into 15 ml Savilex beakers and treated with a mixture of conc. HF/HNO_3 (1:1), 6 M HNO_3 and 6 M HCl. Banded iron formations and manganese crusts (50–250 mg) were treated (1) with aqua regia and (2) with a mixture of HCl/HF (1:1) to digest remaining oxide and silicate phases. Carbonate samples (100–200 mg) were dissolved in 2% HCl. All samples were finally dissolved in 3 M HNO_3. For seawater samples, about 60 ml of the slightly acidified samples (0.1% HCl) was gently heated on a hot plate to reduce its volume to about 15 ml. Concentrated nitric acid was added to the remaining solution to adjust the sample to 3 M HNO_3.

Samples with known U concentrations (including seawater) were spiked prior to digestion. If the U concentration was unknown, an aliquot of ≈10% (precisely weighted) was taken after digestion for U concentration measurements with ICP-MS (ThermoFinnigan Element2 HR-ICP-MS in Frankfurt or X-Series Q-ICP-MS at ASU). Sample concentrations were determined before spiking, to optimize spike/sample ratios.

2.2. Spiking

Prior to chemical separation of U from the matrix, the samples were spiked with a $^{236}U/^{233}U$ mixed isotopic tracer (Chen and Wasserburg, 1981; Stirling et al., 2005; Rademacher et al., 2006) in order to correct for any isotope frac-

tionation on the column and for instrumental mass bias of the MC-ICP-MS. Unlike for other double spike techniques (e.g., Dodson, 1963; Russel et al., 1978; Johnson and Beard, 1999; Siebert et al., 2001), optimizing the spike/sample ratio is not very critical because (1) the mixed isotopic tracer was very pure and well calibrated for the abundances of ^{238}U and ^{235}U and (2) the major spike isotopes, ^{236}U and ^{233}U, do not occur in nature. Thus, analytical precision was not degraded even for high spike/sample ratios, e.g., $^{236}U/^{235}U > 10$. However, we wanted to avoid wasting too much of the valuable U double spike. A minimum amount of spike was necessary for a high-precision measurement (1) to minimize the contribution of amplifier noise and from counting statistics on ^{236}U and ^{233}U on the total uncertainty of the measurement and (2) to minimize the effect of tailing from ^{238}U on ^{236}U, related to the abundance sensitivity of the mass spectrometer. To ensure that the above described effects do not limit the total uncertainty of the U isotope measurement, we used $\pm$constant U_{spike}/U_{sample} ratios on the order of 0.03.

The concentration of the U double spike (13.71 ± 0.04 ppb) was determined by isotope dilution (ID) using two CRM-112A standard solutions (provided from BGS (Parrish et al., 2006) that were diluted from pure U metal (see electronic annex for details of the spike calibration)). The uncertainty on the U concentrations of the CRM-112A solutions was estimated to 1–2‰. However, because ^{236}U and ^{233}U are essentially absent in natural samples, the uncertainty on the spike concentration limits the precision only on the determination of the U concentrations of the samples by ID. It has no effect on the precision of the isotope composition and $\delta^{238}U$ measurements.

The calibration of the spike isotope ratios was performed by (A) measurements of pure spike and (B) measurements of various spike-standard (SRM-950a) mixtures (see electronic annex). With this procedure, the total abundances of the minor spike isotopes could be determined with an uncertainty of ≈2‰ for ^{235}U and <1‰ for ^{238}U, respectively. Because of the very low abundances of these isotopes in the spike (0.05% and 0.15%, respectively), this uncertainty was sufficiently low to have no effect on the precision and accuracy of our samples and standard measurements. Using U_{spike}/U_{sample} ratios of ≈0.03 for the U isotope measurements, results in a contribution of ^{235}U from the spike on ^{235}U of the spike–sample mixture of 0.28% (the contribution of ^{238}U from the spike on ^{238}U of the sample is a factor of 45 smaller). Therefore, an uncertainty of ≈2‰ on ^{235}U of the spike causes an uncertainty on ^{235}U of the sample of at most ≈0.006‰. The precision of the $^{236}U/^{233}U$ of the spike (≈0.05‰) is much higher than the precision of the minor spike isotope ratios. However, its accuracy ultimately depends on the accuracy of the isotope composition we assumed for SRM-950a ($^{238}U/^{235}U = 137.88$: Rosman and Taylor, 1998). Using a more recent value for natural U ($^{238}U/^{235}U = 137.80$: Richter et al., 1999; De Laeter et al., 2003) would result in a slightly different value for the spike $^{236}U/^{233}U$. Fortunately, precise knowledge of the true $^{238}U/^{235}U$ of SRM-950a and of $^{236}U/^{233}U$ of the spike is not critical for the determination of $\delta^{238}U$. Both would only result in a constant offset of the measured $^{238}U/^{235}U$ ratios, but would not reduce the precision or accuracy of measured $\delta^{238}U$ values.

2.3. Chemical separation of U from the sample matrix

Chemical separation of U from the sample matrix was performed with a chromatographic extraction method using Eichrom UTEVA resin modified after Horwitz et al. (1992) and Horwitz et al. (1993). The columns had a volume (cv) of 0.8 ml (ca. 4×0.5 cm). The UTEVA resin was cleaned with 0.05% HCl and then conditioned with 3 cv of 3 M HNO_3 to convert the resin to the nitric form prior to loading the samples (solved in 2–5 ml of 3 M HNO_3) onto the columns. Samples were subsequently rinsed with 16 ml of 3 M HNO_3 to remove most matrix elements from the column, leaving a fraction of U and Th behind. The UTEVA resin was then converted to the chloride form by adding 3 cv of 10 M HCl. Thorium was rinsed from the column with 2×5 cv of a mixture of 5 M HCl and 0.05 M oxalic acid. Subsequently, the columns were rinsed with another 5 cv of 5 M HCl to remove most of the oxalic acid from the column. Uranium was finally eluted with ≈12 cv (e.g., $1 + 1 + 1 + 2 + 5$ ml) of 0.05 M HCl.

Although 100% recovery during purification was not essential (since we used a double spike technique and thus corrected for potential isotope fractionation on the column) chemistry yields were determined by isotope dilution (ID) for a U-standard solution, a seawater sample, a granite and a black shale. For all sample matrices the yield was between 97% and 100%. The U isotope compositions of sample aliquots spiked prior to purification and those spiked after purification were always identical for all sample matrices. To test potential U isotope fractionation on the column we processed a SRM-950a standard solution through the purification procedure. The U eluate was collected in a series of fractions (≈ first 30%, 30–80%, 80–90% and 90–95% of U, eluted with a 1 M instead of a 0.05 M HCl), which were spiked after collection. The U isotope composition of all fractions agreed within ±0.1‰. Thus, obviously no measurable isotope fractionation on the column occurs during elution of U on UTEVA resin with HCl.

The purity of the purified U fractions (for all types of matrices) was checked by ICP-MS. The abundance of all major elements (M), e.g., Ca, Fe, Al, was reduced to $M/U < 1$. The abundance of trace elements (T), which could potentially create argide or hydride interferences (e.g., Pt, Hg, Th) was $T/U < 10^{-3}$. Prior to analyses, samples were treated with 200 µl of a 1:1 mixture of conc. HNO_3 and 32% H_2O_2 on a hot plate to destroy any residual organics, such as very fine particles of resin. Procedure blanks, including digestion and column blanks, were on the order of 10–50 pg, thus more than 3 orders of magnitude lower than the amount of processed U from the samples. Isotope compositions of the blanks were natural within their analytical uncertainties.

2.4. U isotope measurements

Uranium isotope measurements were performed with ThermoScietific Neptune MC-ICP-MS instruments (Weyer

and Schwieters, 2003) at the University of Frankfurt and the Arizona State University. Both instruments were equipped with 9 Faraday detectors and amplifiers with $10^{11}\,\Omega$ resistors. The dynamic range of the amplifier is 50 V and thus suitable for the high-precision measurements of very high (or low) isotope ratios, such as $^{238}U/^{235}U$. Most measurements were performed using a Cetac Aridus combined with a 50 or 100 µl PFA nebulizer for sample introduction. With this setup a 100 ppb U solution was sufficient to achieve a ≈30 V signal on ^{238}U (corresponding to ion yields of 0.5–1%), resulting in a signal of ≈220 mV on ^{235}U. Signals on ^{236}U and ^{233}U were usually ≈400 and ≈600 mV, respectively. Uranium isotope compositions were measured with a total integration time of 5 min. Some measurements were also performed with wet plasma (using an Elemental Scientific SSI spray chamber). However, with this setup, high U concentrations of 400 ppb were necessary to achieve sufficiently high ion beams for high-precision measurements. Within analytical uncertainty, $\delta^{238}U$ values measured with both sample introduction systems agreed with each other (Tables 1 and 2).

Two or three sample measurements were usually bracketed by two standard measurements. Uranium isotope variations of samples and standards are given as $\delta^{238}U$, which is defined as:

$$\delta^{238}U = \left[\frac{(^{238}U/^{235}U)_{sample}}{(^{238}U/^{235}U)_{standard}} - 1\right] \times 1000$$

We reported all U isotope variations relative to the U isotope composition of the standard SRM-950a. We used the daily average $^{238}U/^{235}U$ of this standard for the determination of the delta values between the samples and the standard. Alternatively, the average of the two bracketing standards can also be used (Tables 1 and 2), resulting in (within uncertainties) identical $\delta^{238}U$ values and similar reproducibilities.

The baseline (the electronic noise of the amplifiers) was measured occasionally between two standards (never between sample and standard). Since the noise of the amplifier used for the detection of ^{235}U is one of the limiting factors for the precision of the measurements, we usually performed baseline measurements with the same total integration time as for sample measurements. For such long baseline measurements, the external reproducibility is about 6 µV (2SD), producing an uncertainty on a 200 mV beam (e.g., the ion signal for ^{235}U) of 0.03‰. Measuring the baseline between each sample and standard did not improve the precision of the determined $\delta^{238}U$ values. Sample and standard concentrations were adjusted to ±10%, which limited the influence of the baseline on the precision of the measurement. We also tested to subtract real instrument blanks (measured on clean 2% HNO_3) instead of the amplifier noise. However, this procedure did not change the results of the U isotope measurements. The abundance sensitivity, i.e., the tailing from ^{238}U on ^{236}U was monitored before and after each term of U isotope analyses using an essentially ^{236}U-free standard solution (SRM-950a or CRM-112A). It was usually ≈0.5 ppm, resulting in a contribution of 0.05‰ from the tail of ^{238}U on ^{236}U, if $^{236}U/^{238}U = 0.01$. We applied a correction for this minor tail contribution on the signal measured on mass 236. However, abundance sensitivity did not affect the $\delta^{238}U$ values, as spike/sample ratios were usually kept constant (±10%). The contribution of $^{235}U^{1}H$ to ^{236}U was $<3 \times 10^{-7}$ (for the used spike/sample ratios) and thus did not affect on the measured $^{236}U/^{233}U$. Hydride formation was monitored by measuring $^{238}U^{1}H$ on mass 239. The measured $^{236}U/^{233}U$ and the exponential law (Russel et al., 1978) was used to correct for instrumental mass bias. Mass-independent U isotope fractionation (i.e., nuclear field shift, as briefly discussed below for natural U reduction) appears not to be significant in the plasma source. Otherwise, mass bias corrected $^{238}U/^{235}U$ ratios should correlate with mass bias. However, this was not the case. We replicated SRM-950a (and several other standards and samples) at different days with different instruments (Frankfurt/ASU) and different interface set ups (Aridus, wet plasma), resulting in a range of mass bias on U between ca. 0.5 and 1 a.m.u./mass. However, the variation in mass bias had no effect on the corrected $^{238}U/^{235}U$ ratios.

To verify that variable spike/sample ratios have no influence on the measured U isotope ratios, we measured standard solutions with variable U_{spike}/U_{sample} ratios between 0.016 and 0.133 (Table 1 and Fig. 1). We corrected for the effect of tailing from ^{238}U on ^{236}U (ca. 0.5 ppm: determined prior the U isotope measurements), which was however only essential for the low-spiked standards. By definition, two differently spiked SRM-950a standards measured against each other must have $\delta^{238}U = 0$‰. This was the case within ±0.02‰. As an additional test for our double spike method, we added different amounts of spike to

Table 1
Long term reproducibility of U standards with variable spike–sample ratios

Standard	U_{spike}/U_{sample}	$^{238}U/^{235}U$	2SD	$\delta^{238}U$ (SSB)	2SD (‰)	$\delta^{238}U$ (average)	2SD (‰)	*n*
SRM-950a	0.024–0.031	137.880	0.008					161
SRM-950a	0.018	137.881	0.005	0.00	0.08	0.01	0.08	3
SRM-950a	0.044	137.882	0.008	0.00	0.07	0.01	0.05	3
SRM-950a	0.133	137.878	0.003	−0.03	0.04	−0.02	0.03	2
CRM-112a	0.023–0.026	137.883	0.008	0.01	0.05	0.02	0.05	12
REIMEP-18a	0.016	137.855	0.011	−0.17	0.09	−0.17	0.08	5
REIMEP-18a	0.03–0.04	137.856	0.008	−0.17	0.06	−0.18	0.06	12
REIMEP-18a	0.086	137.856	0.001	−0.17	0.03	−0.18	0.01	2

Standard measurements were performed at the University of Frankfurt and the Arizona State University.

Table 2
Summary of U isotope compositions and concentrations of natural samples

Sample	Material	U-conc	$\delta^{238}U$ (SSB)	2SD	$\delta^{238}U$ (average)	2SD	*n*	$^{238}U/^{235}U$[§]
B7 (Hawaii)[*]	Seawater	3.25	−0.41	0.09	−0.40	0.02	3	137.825
A9 (Hawaii)[*]	Seawater	3.22	−0.41	0.09	−0.41	0.02	3	137.823
B10 (Hawaii)[*]	Seawater	2.93	−0.42	0.13	−0.39	0.10	2	137.826
C7 (Bermuda)[*]	Seawater	3.36	−0.40	0.05	−0.42	0.06	3	137.822
D11 (Bermuda)[*]	Seawater	3.36	−0.41	0.04	−0.42	0.03	3	137.822
D12 (Bermuda)[*]	Seawater	3.37	−0.38	0.04	−0.39	0.05	3	137.826
	Mean seawater	3.25	−0.41	0.03	−0.41	0.03	6	137.824
BCR-2[+]	Basalt	1.67	−0.28	0.08	−0.29	0.07	8	137.840
BEN[+]	Basalt	1.42	−0.31	0.06	−0.33	0.03	5	137.834
BHVO-1 (a)[*]	Basalt		−0.25	0.07	−0.25	0.06	2	137.846
BHVO-1 (b)[*]	Basalt		−0.28	0.01	−0.29	0.00	2	137.840
	Mean basalts		−0.28	0.05	−0.29	0.07	3	137.840
JG-1[+]	Granodiorite	3.93	−0.38	0.07	−0.39	0.09	4	137.826
JG-2[+]	Granite	10.9	−0.33	0.10	−0.33	0.08	4	137.834
G-2[+]	Granite	1.76	−0.21	0.09	−0.20	0.07	3	137.852
NIM-G[*]	Granite	16.65	−0.46	0.01	−0.46	0.06	3	137.817
	Mean granites		−0.35	0.21	−0.35	0.22	4	137.832
Porites[+]	Coral	2.87	−0.40	0.07	−0.40	0.11	4	137.825
Siderastrea (a)[+]	Coral	2.63	−0.42	0.08	−0.44	0.11	4	137.819
Siderastrea (b)[+]	Coral	2.76	−0.43	0.02	−0.46	0.01	3	137.817
Black Sea unit-I								
10-1 (unit-I)[*]	Black shale	16.8	−0.04	0.10	−0.05	0.12	4	137.873
21-1 (unit-I)[*]	Black shale	16.6	−0.03	0.05	−0.02	0.10	3	137.877
21-2 (unit-I)[*]	Black shale	16.8	−0.02	0.00	0.00	0.04	2	137.880
25-1 (unit-I)[*]	Black shale	16.7	0.04	0.01	0.03	0.02	2	137.884
43-1 (unit-I)[*]	Black shale	10.1	0.05	0.06	0.05	0.01	3	137.887
43-2 (unit-I)[*]	Black shale	6.97	−0.06	0.06	−0.04	0.02	2	137.874
55-4 (unit-I)[*]	Black shale	20.7	0.04	0.10	0.06	0.03	2	137.888
	Mean Black Sea unit-I		0.00	0.09	0.00	0.09	12	137.881
Black Sea unit-II								
55-3 (unit-II)[*]	Black shale	12.1	0.43	0.07	0.43	0.06	4	137.939
25-2 (unit-II) (a)[*]	Black shale		0.23	0.10	0.22	0.06	2	137.910
25-2 (unit-II) (b)[*]	Black shale	6.12	0.20	0.04	0.18	0.01	2	137.905
92-763[+]	Kupferschiefer	7.46	0.11	0.08	0.11	0.09	3	137.895
92-763 (wet)[*,†]	Kupferschiefer		0.04	0.06	0.06	0.04	2	137.888
92-765[+]	Kupferschiefer	39.8	0.06	0.06	0.01	0.08	2	137.881
92-766[+]	Kupferschiefer	482	−0.02	0.03	−0.07	0.11	2	137.870
Peru margin								
1H1-42 (42)[*]	Suboxic sediment	12.9	−0.31	0.07	−0.29	0.03	2	137.840
1H1-122 (122)[*]	Suboxic sediment	13.8	−0.18	0.08	−0.15	0.03	2	137.859
1H2-130 (280)[*]	Suboxic sediment	14.0	−0.37	0.09	−0.35	0.06	2	137.832
1H3-22 (322)[*]	Suboxic sediment	9.6	−0.41	0.11	−0.40	0.06	2	137.825
1H4-90 (540)[*]	Suboxic sediment	7.3	−0.16	0.00	−0.16	0.00	2	137.858
1H5-140 (740)[*]	Suboxic sediment	15.6	−0.34	0.03	−0.34	0.01	2	137.833
2H3-70 (1195)[*]	Suboxic sediment	16.2	−0.20	0.13	−0.21	0.14	2	137.851
2H3-130 (1255)[*]	Suboxic sediment	12.3	−0.32	0.11	−0.33	0.11	2	137.834
	Mean suboxic		−0.29	0.19	−0.28	0.19	8	137.842
Mn-A1-core[+]	Manganese nodule	8.03	−0.61	0.07	−0.61	0.05	7	137.796
Mn-A1-core (wet)[*,†]	Manganese nodule		−0.63	0.13	−0.62	0.12	2	137.795
Mn-A1-mid[+]	Manganese nodule	5.83	−0.63	0.06	−0.62	0.03	2	137.795
Mn-A1-rim[+]	Manganese nodule	7.80	−0.60	0.06	−0.62	0.11	5	137.795

(*continued on next page*)

Table 2 (*continued*)

Sample	Material	U-conc	$\delta^{238}U$ (SSB)	2SD	$\delta^{238}U$ (average)	2SD	*n*	$^{238}U/^{235}U$[§]
Mn-A1-rim (wet)[*,†]	Manganese nodule		−0.61		−0.61		1	137.796
A-1[*]	Mangenese crust	3.94	−0.55	0.03	−0.54	0.06	4	137.806
P-1[*]	Mangenese crust	2.50	−0.52	0.06	−0.54	0.10	3	137.806
	Mean manganese crusts		−0.58	0.09	−0.59	0.08	5	137.799
M-2[+]	BIF	0.21	−0.71	0.10	−0.72	0.17	2	137.781
TS-9[+]	BIF	0.16	−0.88	0.02	−0.89	0.08	2	137.757
Mau-1[*]	BIF	0.15	−0.29		−0.29		1	137.840
MaMa-1[*]	BIF	0.18	−0.69	0.06	−0.70	0.14	2	137.783

(a) and (b) indicate analyses of two different splits of the same sample.
[*] U isotope analyses were performed at Arizona State University.
[†] U isotope analyses were performed with wet plasma conditions.
[§] $^{238}U/^{235}U$ ratios are calculated using the $\delta^{238}U$ values of the respective sample and assuming SRM-950a has a $^{238}U/^{235}U$ ratio of 137.88.
[+] U isotope analyses were performed at the University of Frankfurt.

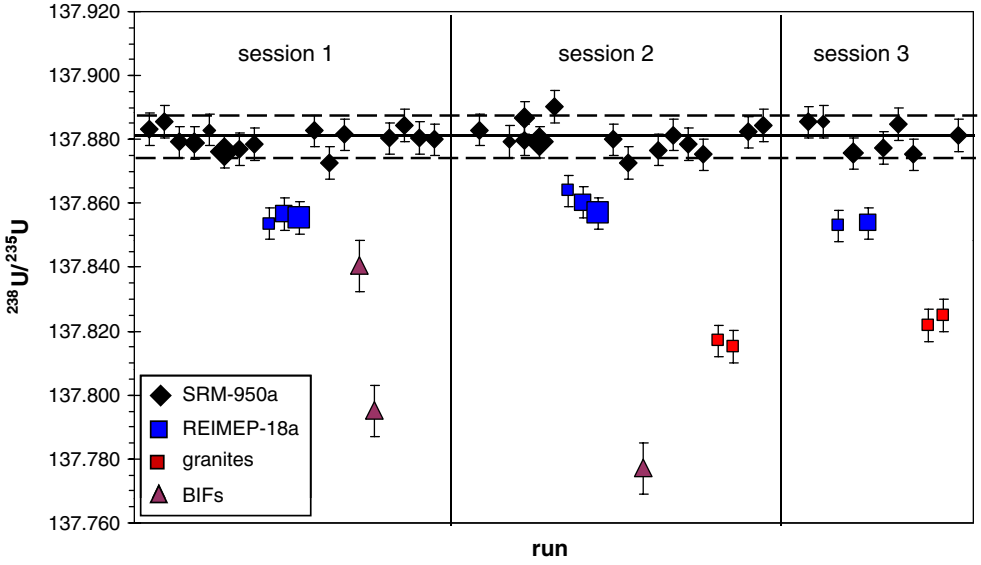

Fig. 1. Three sessions of U isotope measurements (executed within 36 continuous hours) of the U isotope standard SRM-950a (relative to which we report the $\delta^{238}U$ of our samples), another U standard (REIMEP-18a), a granite and three different BIFs. The 2SD reproducibility for SRM-950a of all three sessions together was 0.06‰. Note, the variable symbol sizes for SRM-950a and REIMEP-18a, indicating variable spike/sample ratios between 0.016 and 0.133 (see Table 1) with large symbols for high- and small symbols for low spike/sample ratios.

another U isotope standard, REIMEP-18a (Richter and Wellum, 2006), for which we obtained a slightly different $^{238}U/^{235}U$ ratio. The measured $\delta^{238}U$ of this standard relative to SRM-950a was very reproducible ($\delta^{238}U = -0.17 \pm 0.06$‰), regardless of the spike/sample ratio. This experiment demonstrates that the contribution of ^{235}U and ^{238}U from the spike to the sample was corrected accurately.

3. SAMPLES

For this survey of natural U isotope variations we investigated a variety of different sample types, including 6 seawater samples, 3 basalts, 3 granites and 1 granodiorite, 2 corals, 12 black shales (7 Black Sea unit-I, 2 Black Sea unit-II and 3 Kupferschiefer), 8 suboxic sediments from the Peru continental margin, 3 ferromanganese crusts/nodules and 4 banded iron formations (BIF). The basalts, granites and the granodiorite are international available standards (BCR-2, BEN, BHVO-1, JG-1, JG-2, G-2 and NIM-G).

Of the 6 seawater samples, three each are from Hawaii and Bermuda. The samples were collected with the automated MITESS trace element sampler (Bell et al., 2002) at the Bermuda Testbed Mooring (31.72°N, 64.16°W, August–September 1999) and HALE-ALOHA Mooring (22.45°N, 158.15°W, 36–39 m depth, June–July 1999) sites. Briefly, the sampler opens a 500 ml polyethylene bottle (initially filled with dilute acid) in a trace-metal clean environment, closes it after it is fully flushed and then releases HCl to acidify and preserve the sample at pH 2. The corals (*Porites astreoides* and *Siderastrea sidera*) originate from the Belize islands. They are recent and thus still preserved aragonite crystal structure.

Nine of the 12 black shales we analyzed for this study are from the Black Sea. Seven of them are from unit-I and the other two from unit-II. While unit-I sediments formed under recent conditions, unit-II sediments were deposited during low sea levels and a more restricted flow of Mediterranean waters through the Bosporus (Hay, 1988). The other 3 black shales are ''Kupferschiefer'' from the Zechstein Sea (Europe), which was deposited some 260 Ma ago under euxinic conditions. Ore mineralization (Cu and Zn) occurred in these sediments due to secondary enrichment of these elements during diagenetic processes (Püttmann et al., 1990). These processes probably also lead to secondary U enrichment. All of the suboxic sediments analyzed for this study are from the Peru continental margin. The samples were collected during Ocean Drilling Program (ODP) Leg 112, at Site 680A, which represents an upwelling cell located within the middle of the oxygen minimum zone (OMZ) along the Peru margin. Model ages range from ~1 ky B.P. to ~160 ky.

The ferromanganese oxides we analyzed for this study are the two international standards A-1 (Atlantic) and P-1 (Pacific) and one ferromanganese nodule from the North Atlantic that was provided from the Senckenberg Museum in Frankfurt. After cutting the latter sample into two equal halves, we drilled three samples of a 100 mg each, one of them sampling the core, one the rim and one between core and rim of the manganese crust. The 4 Banded Iron Formation (BIF) samples are from Lake Superior (USA), the Hutti-Maski greenstone belt (Eastern Dharwar Craton, Central India), the Marra Mamba iron formation (Hamersley Group, Western Australia) and from Mauritania (Saouda Group, West African Craton), respectively (e.g., Klein, 1999).

4. RESULTS

For all analyzed samples, precise U concentrations by isotope dilution (ID) were determined along with the U isotope compositions (Tables 1 and 2). The precision of the ID analyses was about 0.2–1% (combining uncertainties from aliquot dilution, the spike calibration and the measurement itself). The reproducibility of SRM-950a U isotope measurements during the term of a measurement was ≈0.05–0.06‰ and daily mean values always agreed within uncertainties (Fig. 2). We measured the U isotope composition of two additional U standards, CRM-112A and REIMEP-18a (Table 1, Fig. 1). While the U isotope composition of CRM-112A is identical to that of SRM-950a to within 0.05‰ (2SD, based on 12 replicate measurements), REIMEP-18a has a slightly negative $\delta^{238}U$ (−0.17‰) relative to SRM-950a. Assuming an isotope composition of $^{238}U/^{235}U = 137.880$ for SRM-950a (Rosman and Taylor, 1998), this corresponds to $^{238}U/^{235}U = 137.856$ for REIMEP-18a. Most of the investigated natural samples display negative $\delta^{238}U$ relative to SRM-950a (Table 2, Fig. 2, see electronic annex for individual analyses). The ranges of U isotopic compositions measured for basalts and granites overlap. However, while the investigated basalts display a tight range of $\delta^{238}U \approx 0.3$‰ within the granite field, the granites display isotopic variations ($\delta^{238}U = -0.20$ to -0.45‰) four times bigger than analytical uncertainties.

All investigated seawater samples (from Hawaii and Bermuda) together display a tight range of U isotope compositions of 0.41 ± 0.03‰. Considering the long residence time of U (≈0.5 Ma: Ku et al., 1977; Cochran et al., 1986; Dunk et al., 2002), the isotopic composition of U

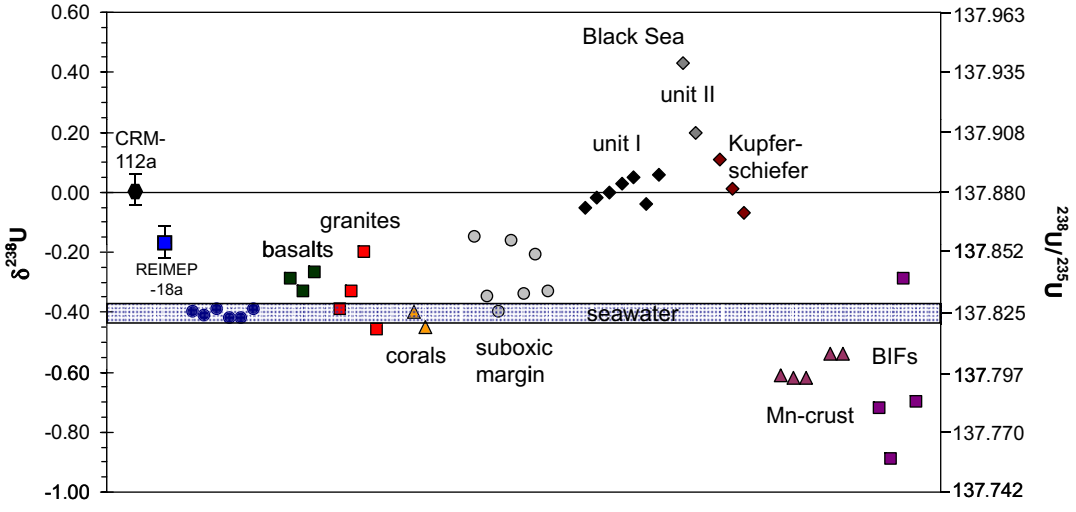

Fig. 2. Summary of delta values for all samples investigated during this study. The dark blue dots within the seawater field represent $\delta^{238}U$ of the individual seawater samples. Significant U isotope fractionation occurs between seawater and black shales (Black Sea, unit-I and -II and Kupferschiefer) which all display heavy U isotope compositions, and between seawater and ferromanganese crusts/nodules and BIFs which all display low $\delta^{238}U$. The low $\delta^{238}U$ of most of the BIFs may also reflect low $\delta^{238}U$ of seawater at the time of their formation (see also text for further discussion). (For interpretation of the references to color in this figure legend, the reader is referred to the web version of this article.)

should be well mixed in the oceans. While samples from Bermuda display an extremely tight range of U concentrations (3.36–3.37 ppb), concentrations of samples from Hawaii are slightly lower and more variable (2.93–3.25 ppb). The concentration difference is beyond analytical precision, which is demonstrated by the reproducibility of the Bermuda samples (≈0.2%). The lower U concentration of two of the Hawaii samples (3.22 and 3.25 ppb) compared to that of the Bermuda samples is consistent with typical salinity differences (≈4%) between the two regions (Schroeder and Stommel, 1969; Bingham and Lukas, 1996). The low U concentration of one Hawaii sample is inconsistent with a constant U/salinity ratio (Chen et al., 1986a; Robinson et al., 2004; Andersen et al., 2007) and we suspect incomplete sample bottle flushing as the cause of this low U concentration. The two investigated corals, display $\delta^{238}U \approx -0.43‰$, which is identical to the $\delta^{238}U$ of seawater within uncertainties. The uniform U isotope composition of seawater and corals is consistent with findings of Stirling et al. (in press). However, contrary to these authors, we observed slightly lighter U isotope compositions (outside analytical uncertainties) for both seawater and corals compared to basalts.

The investigated manganese crusts displayed generally light isotope compositions ($\delta^{238}U$ values of −0.54 to −0.62‰) compared to seawater (consistent with Stirling et al., in press). Uranium concentrations of these samples vary between 2.5 and 8 ppm. The lightest U isotope compositions were observed for three BIFs (Lake Superior, Marra Mamba and Central India) with $\delta^{238}U = -0.72‰$, −0.70‰ and −0.89‰, respectively. The uncertainty on $\delta^{238}U$ for the BIFs is higher than for other samples (0.1–0.2‰) because of their low U concentrations (0.15–0.2 ppm) and resultant lower ion beam intensities during U isotope measurements. Only one of the investigated BIFs ($\delta^{238}U = -0.29‰$) is significantly heavier than the others. In contrast, the black shale samples (Black Sea and Kupferschiefer) all have significantly heavier $\delta^{238}U$ values of −0.05 to +0.43‰. Two unit-II sediments from the Black Sea are particularly heavy, with $\delta^{238}U = +0.20‰$ and +0.43‰, respectively. The other black shales display significantly less isotopic variation, e.g., all of the 7 analyzed Black Sea unit-I sediments fall within a tight range of $\delta^{238}U = -0.05‰$ to +0.06‰. The suboxic sediments from the Peru margin as well as the investigated carbonates have U isotope compositions between those of black shales and seawater (−0.13‰ to −0.40‰). The range of U concentrations is similar for the investigated suboxic margin sediments and black shales (≈6–21 ppm).

Long term reproducibility for $\delta^{238}U$ of our U standards (CRM-112A and REIMEP-18a) was ≈0.05–0.06‰ (2SD). However, we analyzed most samples three times or more. The resulting mean value of such replicate sample measurements should be more precise than replicates of single measurements (assuming a Student-*t* distribution, e.g., Weyer et al., 2005). Indeed, this is indicated by some sample groups, which are supposed to have an invariant U isotope composition, such as seawater. All analyzed seawater samples together display U isotope variations of only ±0.03‰ (2SD). These results demonstrate the precision attainable with our method on natural samples. Other groups of samples, such as the Black Sea unit-I sediments and the basalts, also define a tight range of U isotope compositions of only 0.05‰ and 0.09‰, respectively. While Black Sea unit-I samples probably display real variations, the basalts should also be expected to have a constant U isotope compositions (Stirling et al., 2005, in press), although small variations can not be excluded. The total range in $\delta^{238}U$ we observed in this study from the isotopically lightest to the heaviest sample was ≈1.3‰, exceeding by far our analytical precision. Assuming $^{238}U/^{235}U = 137.880$ for SRM-950a (Rosman and Taylor, 1998). This range in $\delta^{238}U$ corresponds to a range of $^{238}U/^{235}U$ from 137.757 to 137.939.

5. DISCUSSION

5.1. U isotope fractionation during the reduction of U^{VI} to U^{IV}

The largest isotope variations found in our survey are between oxidized and reduced depositional environments, with seawater and suboxic sediments falling in between (Figs. 2 and 3). Therefore, U redox transformations appear to be important in U isotope fractionation. We find that the heaviest U isotope compositions are generally observed for black shales ($\delta^{238}U$ of −0.05‰ to +0.43‰), which contain the reduced form of U (Table 2 and Fig. 2). If we consider typical black shales such as Black Sea unit-I ($\delta^{238}U = -0.05‰$ to +0.06‰), this corresponds to U isotope fractionation of ≈0.4‰ during U reduction from seawater ($\delta^{238}U = -0.41$).

What is the origin of this isotope fractionation? Many studies predict that microorganisms play a role during the reduction of dissolved U^{VI} (which exists in ocean water as carbonate complexes of uranyl) to insoluble UO_2 (Barnes and Cochran, 1990; Klinkhammer and Palmer, 1991; Lovely et al., 1991; Lovley, 1993; Wersin et al., 1994; Suzuki and Banfield, 1999; Zheng et al., 2002b). This might be the case even in anoxic environments (Anderson et al., 1989; Colodner et al., 1995). Recently, the effect of microbial reduction on U isotopes was experimentally investigated (Rademacher et al., 2006). These authors observed an increase in $\delta^{238}U$ of the unreacted U^{VI} with decreasing uranium concentration due to bacterial reduction by *Geobacter sulfurreducens* and *Acetobacterium dehalogenans*, indicating that light U isotopes (^{235}U) are preferentially removed from solution during reduction. Rademacher et al. (2006) interpreted their results as evidence of kinetic isotope fractionation leading to an enrichment of light isotopes in the reaction product. However, our data suggest that reduction of U^{VI} species in marine sedimentary environments fractionates U isotopes in the opposite sense, producing isotopically heavy reduced U. Hence, our data are not easily explained by a microbially-mediated kinetic isotope effect.

Instead, the magnitude and direction of fractionation we observe is consistent with theoretical predictions of Schauble (2006, 2007), who modeled nuclear volume effects on stable isotope fractionation for some very heavy elements, including U. At equilibrium, volume-dependent fractionation is predicted to be a factor of ≈2 larger than mass-

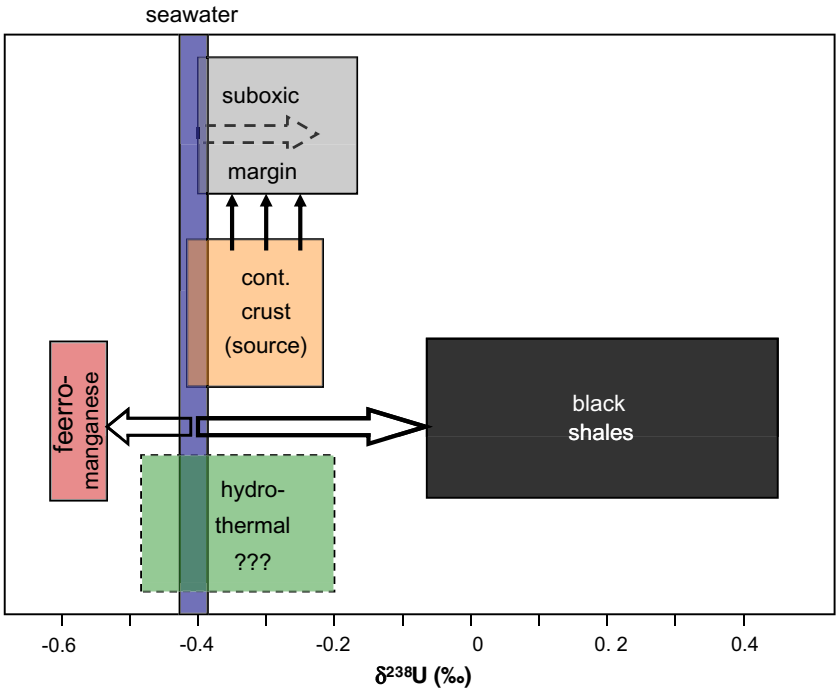

Fig. 3. Preliminary box model for U isotope fractionation within the ocean cycle, based on the ranges of U isotope compositions for the various reservoirs. Note that the range for the hydrothermal sink was estimated based on mass balance considerations. The ranges of U isotope compositions for all other sources and sinks are based on measurements of this study (see text for further discussion).

dependent fractionation. Further, this theory predicts that reduced U species (U^{IV}) should preferentially incorporate the heavy U isotopes, contrary to expectations from classic mass-dependent fractionation (Schauble, 2004). The net fractionation between U^{IV} and U^{VI} species is predicted to be on the order of 1‰ for $^{238}U/^{235}U$ (Schauble, 2006), with U^{IV} species isotopically heavier. Both the direction and magnitude of this prediction are in reasonable agreement with our observations. We therefore interpret our data as the result of volume-dependent equilibrium isotope fractionation. It is interesting to point out that, because of the nuclear volume effect, the U isotope system is unique in permitting us to easily differentiate between equilibrium and kinetic isotope effects during reduction.

The U isotope compositions of suboxic margin sediments (from the Peru margin) are heavier than, but relatively close to, the seawater value. Thus, there is a systematic difference between suboxic and euxinic sediments (Figs. 2 and 3). The reason for the differences in $^{238}U/^{235}U$ among different types of reduced sediments is not clear. Suboxic sediments are defined by their low oxygen concentrations in the bottom water (e.g., 0.2–2 ml O_2 in 1 l H_2O: Tyson and Pearson, 1991), while euxinic sediments accumulate in the presence of free H_2S in the water column and the effective absence of oxygen (Tyson and Pearson, 1991). The mechanisms of U removal in these different settings are not well understood and may result in different isotope effects. Multiple processes, such as precipitation and remobilization of U, may be important for suboxic sediments (Morford and Emerson, 1999; Zheng et al., 2002a; McManus et al., 2005) and produce some of the observed scatter in U isotope fractionation of the margin sediments. Alternatively, differences between suboxic and euxinic sediments may arise from the fact that suboxic margin sediments typically become more reducing below the sediment–water interface (Klinkhammer and Palmer, 1991; Morford and Emerson, 1999; McManus et al., 2005). In this case, U is reduced and precipitated at a certain depth (together with other redox-sensitive elements, such as Mo and Re). Uranium removal from sediment porewaters under these conditions is very effective (Klinkhammer and Palmer, 1991; McManus et al., 2005), which may result in little expressed fractionation due to mass balance constraints.

5.2. U isotope fractionation during incorporation of U into manganese crusts

The ferromanganese crusts and nodules that we analyzed display light isotope compositions compared to modern seawater. ($\delta^{238}U = -0.54‰$ to $-0.62‰$), implying isotope fractionation of $\approx -0.1‰$ to $-0.2‰$ during incorporation of U from seawater into these sediments (Table 2, Figs. 2 and 3). This fractionation is reminiscent of the Mo isotope system, in which Mo associated with ferromanganese crusts is also isotopically light compared to seawater (Barling et al., 2001; Siebert et al., 2003; Anbar, 2004; Barling and Anbar, 2004) (Fig. 4). However, U isotope fractionation is much weaker in these environments. Thallium isotopes also strongly fractionate during incorporation to ferromanganese sediments, but in an opposite sense (Rehkämper et al., 2002, 2004) (Fig. 4).

Isotope fractionation of both Mo and Tl have been explained as resulting from equilibrium fractionation during

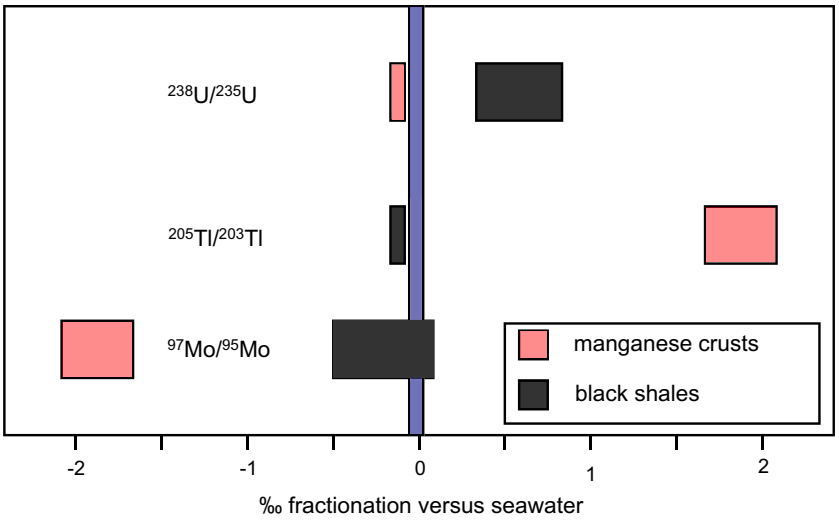

Fig. 4. A comparison of $^{238}U/^{235}U$, $^{97}Mo/^{95}Mo$, and $^{205}Tl/^{203}Tl$ isotope fractionations between seawater, ferromanganese crusts and black shales (anoxic/euxinic sediments). Molybdenum and Tl isotope data are taken from Arnold et al. (2004), Barling et al. (2001), Rehkämper et al. (2002, 2004) and Siebert et al. (2003) (see text for further discussion).

adsorption onto Mn-oxide surfaces (Barling et al., 2001; Rehkämper et al., 2002; Anbar, 2004; Barling and Anbar, 2004; Rehkämper et al., 2004) or between two species in solution, with only one adsorbing to the surface (e.g., Siebert et al., 2003). Kinetic isotope effects cannot be completely excluded for Mo isotopes, since the adsorbed Mo is isotopically light. Similarly to Mo, the predominant species of U in seawater are negatively charged complexes (carbonate complexes in case of U and oxyanions in case of Mo), while Tl mainly occurs as the cations Tl^{+} and Tl^{3+}. These differences in speciation may account for the different direction of Mo and U compared to Tl isotope fractionation during incorporation into ferromanganese crusts. However, none of the above discussed mechanisms can be currently excluded for U. Experimental and theoretical studies are both needed to better understand U isotope fractionation in oxic marine systems.

5.3. The U isotope ocean budget

The major source and sink of U to and from the oceans are believed to be the continental crust and organic-rich suboxic continental margin sediments, respectively (e.g., Morford and Emerson, 1999). This model implies that suboxic margin sediments should have a U isotope composition very similar to the crust (as represented in this study by average granites + basalts), assuming that no U isotope fractionation occurs during weathering and transport of U to the oceans. In fact, this is precisely what we observe, with both having $\delta^{238}U \approx -0.3‰$ (Fig. 3). Although isotope fractionation is observed in both black shales and ferromanganese crusts, neither type of sediment is very important to the oceanic U budget. Hence, our isotopic data are consistent with present understanding of the oceanic U budget. The only significant U sink not considered in this study is U removal at hydrothermal vent sites and during alteration of oceanic crust (Chen et al., 1986b; Morford and Emerson, 1999). No U isotope data yet exist from those sites. However, mass balance considerations require that this sink does not strongly fractionate U isotopes; otherwise suboxic sediments would be offset from crustal sources (Fig. 3).

Notably, U in seawater ($\delta^{238}U = -0.41‰$) appears to be slightly lighter than in either the crust or suboxic sediments (Figs. 2 and 3). This small isotope offset may be produced by the small fractionation during incorporation into suboxic sediments. However, euxinic depositional environments, although only a minor sink for U at present, may also contribute to the observed isotopic shift in seawater because heavy U isotopes are strongly enriched in sediments accumulating in such environments. Due to this difference between suboxic and euxinic environments, the U isotope composition of seawater may be sensitive to perturbations in the relative importance of different U sinks. During epochs of more widespread euxinic conditions, the relative importance of euxinic environments as a U sink should increase, which may result in a more fractionated (lighter) seawater U isotope composition. However, if U isotope fractionation during weathering occurs and is sensitive to specific weathering conditions (e.g., climate), variations in the U isotopic composition of the sources to the oceans may occur and also be recorded in seawater. Hence, variations in seawater U isotope compositions may be a novel means to study changes in ocean redox conditions, and/or in weathering intensity and sources in geologically-recent times.

This approach would be similar to that of Arnold et al. (2004) who used variations in the Mo isotope composition between modern and Proterozoic seawater (represented by Proterozoic black shales) to reconstruct paleo-redox conditions. Although Mo and U are both redox-sensitive metals and display similar behavior in the ocean, cycle, e.g., they are both enriched in euxinic sediments (e.g., Colodner et al., 1995; Algeo and Maynard, 2004; Tribovillard et al.,

2006), they display contrasting isotope systematics in both magnitude and direction in oxic and euxinic environments (Fig. 4). In euxinic environments, U isotopes are strongly fractionated toward heavier isotope compositions, but little or even no Mo isotope fractionation is observed under these conditions (Barling et al., 2001). The latter was explained by the authors to result from virtually quantitative removal of Mo from the water column under euxinic conditions (with $H_2S > 100$ μM, Helz et al., 1996). Uranium is not incorporated into sulfides and a quantitative removal of U in euxinic environments does not occur. The latter is indicated by U concentration profiles of the Black Sea water column (Colodner et al., 1995) and supported by the strong U isotope fractionation we observed in Black Sea black shales. Probably, U removal is restricted to the sediments, while Mo may be partially removed in the water column (Colodner et al., 1995). On the other hand, in oxic and suboxic environments (which are the major present-day sinks for Mo and U, respectively), only little U isotope fractionation occurs, while Mo displays particularly large isotope fractionation under oxic conditions (e.g., during adsorption to ferromanganese oxides) and also variable isotope fractionation in suboxic environments (Siebert et al., 2006).

These different isotope systematics for Mo and U may result in opposite effects during a global change in redox conditions. Thus, combining Mo and U isotope compositions may be an interesting approach to investigating global paleo-redox changes. Uranium isotope variations of paleo-seawater may be recorded by some fossils as indicated by the identical $\delta^{238}U$ of corals and seawater. However, further studies of the U isotope compositions of fossils are necessary to evaluate which fossils can serve as reliable recorders of paleo-redox conditions.

Intriguingly, the U isotope compositions in three of four BIF samples are significantly lighter than in recent ferromanganese crusts, and altogether the BIF samples span a wider range of values than seen in modern crusts (Table 2 and Fig. 2). The lighter values could indicate that a larger fractionation occurs during adsorption or co-precipitation of U into ferric oxyhydroxides, as opposed to manganese oxides. Alternatively, the U isotope composition of the oceans may have been different during the Archean, either as a result of fractionation that might have occurred during U weathering and transport under an anoxic atmosphere or due to different redox conditions of the Archean oceans that affected the oceanic U isotope budget. In the latter case, predominantly anoxic conditions may have resulted in preferential removal of heavy U isotopes from the oceans and thus generated isotopically light seawater. Anoxic conditions should also result in low U concentrations of the Archean oceans, which is consistent with the very low U concentrations that we observed in BIFs and in contrast to modern ferromanganese crusts.

5.4. The effect of U isotope fractionation on U–Pb dating

It is beyond the scope of this study (1) to provide a full consideration of the effect of variable U isotope compositions on U–Th–Pb dating and (2) to discuss the accuracy of the recommended and universally used value for the present-day $^{238}U/^{235}U$ (137.80–137.88: Rosman and Taylor, 1998; De Laeter et al., 2003). However, we point out that any isotope fractionation of U before or during the decay of U to Pb may result in apparent age variations of cogenetic samples. While the bias in the calculated ^{238}U–^{206}Pb ages depends on the analytical technique (i.e., mass bias correction), U isotope fractionation has a direct effect on $^{207}Pb/^{206}Pb$ ages which is briefly discussed below. The effect on U-series dating is discussed in detail by Stirling et al. (in press).

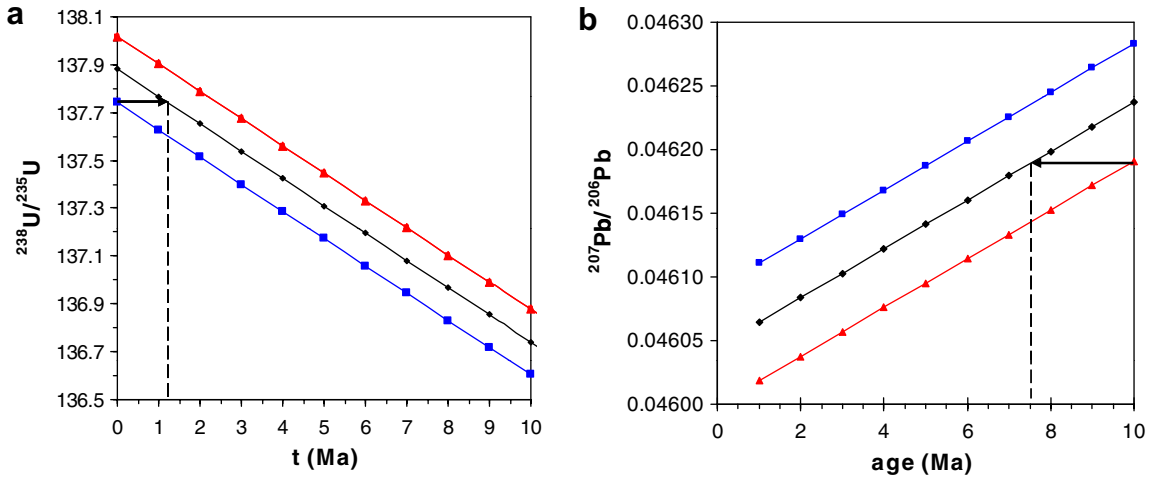

Fig. 5. (a) Evolution of the $^{238}U/^{235}U$ isotope ratio: during the last 10 Ma. Also shown is the U isotope evolution of two minerals that are fractionated against present-day $^{238}U/^{235}U = 137.88$ by +1‰ (line with squares) and −1‰ (line with triangles), respectively. One per-mil U isotope fractionation is equal to 1.2 Ma of U isotope evolution (with time). (b) Effect of variable U isotope compositions (+1‰ and −1‰, symbols like in Fig. 5a) on Pb–Pb dating. Isotopically light minerals would produce systematically higher $^{207}Pb/^{206}Pb$ ages (>2 Ma for 1‰ U isotope fractionation). This effect is stronger for young than for old minerals (see text for further discussion).

During Earth's history, radioactive decay has caused the U isotope composition to change dramatically, from an initial $^{238}U/^{235}U$ of ≈3.1 to the present-day value. The relative change (increase) of $^{238}U/^{235}U$ with time is constant and about 0.83‰ per Ma (Fig. 5a). Thus, the total spread of U isotope variations observed in this study is equivalent to about 1.6 Ma of U isotope evolution. Variable U isotope compositions of minerals that are used for U–Pb dating may result in apparent age differences of significant magnitude if applying $^{207}Pb/^{206}Pb$ dating (Fig. 5b). For example, if two cogenetic 3 Ga zircons had U isotope compositions that differed by 1‰ at the time of formation, they would have an apparent $^{207}Pb/^{206}Pb$ age difference of 1.6 Ma (or 0.5 ‰). Two young zircons (e.g., ≈10 Ma), also with $\Delta^{238}U$ of 1‰, will have an apparent $^{207}Pb/^{206}Pb$ age difference of 2.4 Ma, or 24%.

Due to the lack of high-precision U isotope analyses of datable phases we can only speculate about how much U isotope fractionation really occurs in minerals commonly used for U–Pb geochronology. Generally, U isotope fractionation should be more pronounced for low-temperature mineral phases (e.g., apatite, rutile, sphene, hydrothermal zircons or carbonates). However, significant U isotope variations might also occur in high-temperature metamorphic complexes if their precursor rocks are near-surface sediments with highly fractionated U isotope compositions. For Fe, such large isotope variations within high-grade rocks (Akilia Islands, Greenland) were observed by Dauphas et al. (2004) and interpreted by the authors as inherited signatures from precursor sediments (BIFs). If we assume that the total range of U isotope variations observed in nature is covered by a mineral which is used for dating, this would produce age variations of up to 3 Ma. However, even if U isotope variations are much smaller (e.g., 0.26‰, the range we observed for granites), this would still produce apparent variations in the $^{207}Pb/^{206}Pb$ age of 0.63 Ma for very young zircons (and 0.42 Ma for 3 Ga old zircons). Thus, high-precision U–Pb dating (Bowring et al., 1998; Martin et al., 2000; Condon et al., 2005), particularly of young zircons and other accessory U-bearing minerals, may be limited by natural variations of the U isotope composition.

6. CONCLUSIONS

High-precision U isotope analyses have been performed on a variety of natural samples, including basalts, granites, carbonates, corals, seawater, black shales, suboxic margin sediments, ferromanganese crusts and BIFs (Table 2 and Fig. 2). Our results demonstrate that U isotope fractionation occurs in nature, and hence that the field of "stable" isotope geochemistry spans the periodic table, from H to U.

The most significant U isotope fractionation occurs during U reduction in anoxic/euxinic environments. This is indicated by large $\Delta^{238}U$ of black shales relative to seawater (up to +0.84‰). A much smaller but resolvable fractionation (also toward heavier isotope compositions) appears to occur during U removal in suboxic environments. In oxic environments, U isotopes are fractionated toward lower $\delta^{238}U$ during incorporation into ferromanganese crusts ($\Delta^{238}U_{seawater-Mn\text{-}crust} \approx -0.13‰$ to $-0.21‰$). The lightest U isotope compositions are seen in three BIFs (−0.70‰ to −0.89‰) which may reflect particularly strong fractionation of light U isotopes to the BIFs or differences in the U isotope budget of Archean oceans, or Archean weathering conditions, compared to today. The light U isotope composition of the Hutti-Maski BIF together with the heavy U isotope composition of a Black Sea unit-II black shale together span a range of 1.3‰, representing the maximum range of naturally observed U isotope variations.

The magnitude and direction of U isotope fractionation during U reduction is in agreement with theoretical calculations of volume-dependent fractionation (Schauble, 2006). They are of opposite direction to expectations from classic mass-dependent fractionation or from recently observed kinetic U isotope fractionation during microbial reduction (Rademacher et al., 2006). Hence, our findings provide evidence that volume-dependent effects are important in nature. A number of applications of this isotope system are likely to emerge:

(1) In view of the importance of this element to industrial economies and to international security, U isotopic studies in the environment may provide valuable new information about U sources and the processes affecting U transport.
(2) Because of the opposite fractionation behavior in euxinic and oxic environments, U isotope compositions may provide novel means to study paleo-redox conditions in geological environments.
(3) Since the relative importance of euxinic sinks probably increased during epochs of more reduced paleooceans, seawater U isotope compositions may have changed with time. Thus, U isotope compositions of sediment and fossil recorders may be a promising new tracer for tracking the global evolution of paleo-redox conditions through time.
(4) The results of this study further imply that the U isotope variations of U-bearing minerals that are used for U–Pb dating may be of sufficient magnitude to affect the precision of U–Pb dating. For example, per-mil level variations in the U isotope composition would produce an apparent offset in the $^{207}Pb/^{206}Pb$ age of >1 Ma and thus may limit the precision of the Pb–Pb ages.

ACKNOWLEDGMENTS

We thank G. Ravizza for providing Black Sea black shales, Wilhelm Püttmann and Soodabeh Durali-Müller for providing Kupferschiefer samples, Eberhardt Gischler for providing coral samples, the Senckenberg Museum in Frankfurt for providing a manganese nodule and Ulf Linnemann, Alan Woodland and Alexander Schmidt for providing samples from banded iron formations. Gail Arnold and Klaus Mezger are thanked for helpful discussion and Anna Neumann for laboratory assistance. We thank Gideon Henderson, Claudine Stirling and an anonymous reviewer for their constructive reviews. Jim McManus is thanked for editorial handling. This work was supported by grants from the US National Science Foundation (Geobiology & Low Temperature Geochemis-

try and Instrumentation & Facilities programs) and NASA (Exobiology program) to A.D.A.

APPENDIX A. SUPPLEMENTARY DATA

Supplementary data associated with this article can be found, in the online version, at doi:10.1016/j.gca.2007.11.012.

REFERENCES

Albarede F. (2004) The stable isotope geochemistry of copper and zinc. In *Geochemistry of Non-traditional Stable Isotopes*, vol. 55 (eds. C. M. Johnson and B. L. Beard). Mineralogical society of America, pp. 409–427.

Algeo T. J. and Maynard J. B. (2004) Trace-element behavior and redox facies in core shales of Upper Pennsylvanian Kansas-type cyclothems. *Chem. Geol.* **206**(3–4), 289–318.

Anbar A. D. (2004) Molybdenum stable isotopes: observations, interpretations and directions. In *Geochemistry of Non-traditional Stable Isotopes*, vol. 55 (eds. C. M. Johnsons, B. L. Beard and F. Albarede). pp. 429–450.

Andersen M. B., Stirling C. H., Porcelli D., Halliday A. N., Andersson P. S. and Baskaran M. (2007) The tracing of riverine U in Arctic seawater with very precise U-234/U-238 measurements. *Earth Planet. Sci. Lett.* **259**(1–2), 171–185.

Anderson R. F. (1987) Redox behavior of uranium in an anoxic marine basin. *Uranium* **3**(2–4), 145–164.

Anderson R. F., Fleischer M. Q. and LeHuray A. P. (1989) Concentration, oxidation state and particle flux of uranium in the Black Sea. *Geochim. Cosmochim. Acta* **53**, 2215–2224.

Arnold G. L., Anbar A. D., Barling J. and Lyons T. W. (2004) Molybdenum isotope evidence for widespread anoxia in Mid-Proterozoic oceans. *Science* **304**, 87–90.

Barling J. and Anbar A. D. (2004) Molybdenum isotope fractionation during adsorption by manganese oxides. *Earth Planet. Sci. Lett.* **2217**, 315–329.

Barling J., Arnold G. L. and Anbar A. D. (2001) Natural mass dependent variations in the isotope compositions of molybdenum. *Earth Planet. Sci. Lett.* **193**, 447–457.

Barnes C. E. and Cochran J. K. (1990) Uranium removal in oceanic sediments and the oceanic U balance. *Earth Planet. Sci. Lett.* **97**, 94–101.

Bell J., Betts J. and Boyle E. (2002) MITESS: a moored in situ trace element serial sampler for deep-sea moorings. *Deep-Sea Res. I: Oceanogr. Res. Pap.* **49**(11), 2103–2118.

Bergquist B. A. and Blum J. D. (2007) Mass-dependent and -independent fractionation of Hg isotopes by photoreduction in aquatic systems. *Science* **318**, 417–420.

Bigeleisen J. (1996) Temperature dependence of the isotope chemistry of the heavy elements. *Proc. Natl. Acad. Sci.* **93**, 9393–9396.

Bingham F. M. and Lukas R. (1996) Seasonal cycles of temperature, salinity and dissolved oxygen observed in the Hawaii Ocean time-series. *Deep-Sea Res. II: Top. Stud. Oceanogr.* **43**(2–3), 199–213.

Bowring S. A., Erwin D. H., Jin Y. G., Martin M. W., Davidek K. and Wang W. (1998) U/Pb zircon geochronology and tempo of the end-Permian mass extinction. *Science* **280**(5366), 1039–1045.

Calvert S. E. and Pedersen T. F. (1993) Geochemistry of recent oxic and anoxic marine-sediments—implications for the geological record. *Mar. Geol.* **113**(1–2), 67–88.

Chen J. H., Edwards R. L. and Wasserburg G. J. (1986a) U-238, U-234 and Th-232 in seawater. *Earth Planet. Sci. Lett.* **80**(3–4), 241–251.

Chen J. H., Wasserburg G. J., Vondamm K. L. and Edmond J. M. (1986b) The U–Th–Pb systematics in hot-springs on the east Pacific rise at 21-degrees-N and Guaymas-basin. *Geochim. Cosmochim. Acta* **50**(11), 2467–2479.

Chen J. H. and Wasserburg G. J. (1981) Isotopic determination of uranium in picomole and subpicomole quantities. *Anal. Chem.* **53**, 2060–2067.

Cochran J. K., Carey A. E., Sholkovitz E. R. and Suprenant L. D. (1986) The geochemistry of uranium and thorium in coastal marine sediments and sediment porewaters. *Geochim. Cosmochim. Acta* **50**, 663–680.

Colodner D., Edmond J. and Boyle E. (1995) Rhemium in the Black Sea: comparison with molybdenum and uranium. *Earth Planet. Sci. Lett.* **131**, 1–15.

Condon D., Zhu M. Y., Bowring S., Wang W., Yang A. H. and Jin Y. G. (2005) U–Pb ages from the neoproterozoic Doushantuo Formation, China. *Science* **308**(5718), 95–98.

Cowan G. A. and Adler H. H. (1976) The variability of the natural abundance of 235U. *Geochim. Cosmochim. Acta* **40**, 1487–1490.

Dauphas N., van Zuilen M., Wadhwa M., Davis A. M., Marty B. and Janney P. E. (2004) Clues from Fe isotope variations on the origin of early Archean BIFs from Greenland. *Science* **306**, 2077–2080.

De Laeter J. R., Bohlke J. K., De Bievre P., Hidaka H., Peiser H. S., Rosman K. J. R. and Taylor P. D. P. (2003) Atomic weights of the elements: review 2000—(IUPAC technical report). *Pure Appl. Chem.* **75**(6), 683–800.

Dodson M. H. (1963) A theoretical study of the use of internal standards for precise isotopic analysis by the surface ionization technique: Part I general first-order algebraic solutions. *J. Sci. Instrum.* **40**, 289–295.

Dunk R. M., Mills R. A. and Jenkins W. J. (2002) A reevaluation of the oceanic uranium budget for the Holocene. *Chem. Geol.* **190**, 45–67.

Halliday A. N., Lee D. C., Christensen J. N., Rehkamper M., Yi W., Luo X. Z., Hall C. M., Ballentine C. J., Pettke T. and Stirling C. (1998) Applications of multiple collector-ICPMS to cosmochemistry, geochemistry, and paleoceanography. *Geochim. Cosmochim. Acta* **62**(6), 919–940.

Hay B. J. (1988) Sediment accumulation in the central western Black Sea over the past 5 100 years. *Paleoceanography* **3**, 491–508.

Helz G. R., Miller C. V., Charnock J. M., Mosselmans J. F. W., Pattrick R. A. D., Garner C. D. and Vaughn D. J. (1996) Mechanism of molybdenum removal from the sea and its concentration in black shales: EXAFS evidence. *Geochim. Cosmochim. Acta* **60**, 3631–3642.

Henderson G. M., Slowey N. C. and Fleisher M. Q. (2001) U–Th dating of carbonate platform and slope sediments. *Geochim. Cosmochim. Acta* **65**(16), 2757–2770.

Horwitz E. P., Chiarizia R., Dietz M. L. and Diamond H. (1993) Separation and preconcentration of actinides from acidic media by extraction chromatography. *Anal. Chim. Acta* **281**, 361–372.

Horwitz E. P., Dietz M. L., Chiarizia R. and Diamond H. (1992) Separation and preconcentration of uranium from acidic media by extraction chromatography. *Anal. Chim. Acta* **266**, 25–37.

Johnson C. M. and Beard B. L. (1999) Correction of instrumentally produced mass fractionation during isotopic analysis of Fe by thermal ionization mass spectrometry. *Int. J. Mass Spectrom.* **193**, 87–99.

Johnson C. M., Beard B. L., Roden E. E., Newman D. K. and Nealson H. (2004) Isotope constraints on biogeochemical cycling of Fe. In *Geochemistry of Non-traditional Stable Isotopes*, vol. 55 (eds. C. M. Johnson and B. L. Beard). pp. 359–407.

Johnson T. M. and Bullen T. D. (2004) Mass-dependent fractionation of selenium and chromium isotope in low-temperature

environments. In *Geochemistry of Non-traditional Stable Isotopes*, vol. 55 (eds. C. M. Johnson, B. L. Beard and F. Albarede). pp. 289–317.

Klein C. (1999) Some Precambrian banded iron-formations (BIFs) from around the world: their age, geologic setting, mineralogy, metamorphism, geochemistry, and origin. *Am. Mineral.* **90**, 1473–1499.

Klinkhammer G. P. and Palmer M. R. (1991) Uranium in the oceans: where it goes and why. *Geochim. Cosmochim. Acta* **55**, 1799–1806.

Kronberg J. (1974) Uranium deposition and Th-234 alpha recoil: an explanation for extreme U-234/U-238 fractionation within the Trinity aquifer. *Earth Planet. Sci. Lett.* **21**, 327–330.

Ku T.-L., Knauss K. and Mathieu G. G. (1977) Uranium in the open ocean: concentration and isotopic composition. *Deep Sea Res.* **24**, 1005–1017.

Langmuir D. (1978) Uranium solution-mineral equilibria at low temperatures with applications to sedimentary ore deposits. *Geochim. Cosmochim. Acta* **42**, 547–569.

Lovely D. R., Phillips E. J. P., Gorby J. A. and Landa E. R. (1991) Microbial reduction of uranium. *Nature* **350**, 413–416.

Lovley D. R. (1993) Dissimilatory metal reduction. *Annu. Rev. Microbiol.* **47**, 263–290.

Maréchal C. N., Telouk P. and Albarede F. (1999) Precise analysis of copper and zinc isotopic compositions by plasma-source mass spectrometry. *Chem. Geol.* **156**, 251–273.

Martin M. W., Grazhdankin D. V., Bowring S. A., Evans D. A. D., Fedonkin M. A. and Kirschvink J. L. (2000) Age of Neoproterozoic bilatarian body and trace fossils, White Sea, Russia: implications for metazoan evolution. *Science* **288**(5467), 841–845.

McManus J., Berelson W. M., Klinkhammer G. P., Hammond D. E. and Holm C. (2005) Authigenic uranium: relationship to oxygen penetration depth and organic carbon rain. *Geochim. Cosmochim. Acta* **69**, 95–108.

McManus J., Berelson W. M., Severmann S., Poulson R. L., Hammond D. E., Klinkhammer G. P. and Holm C. (2006) Molybdenum and uranium geochemistry in continental margin sediments: Paleoproxy potential. *Geochim. Cosmochim. Acta* **70**(18), 4643–4662.

Morford J. L. and Emerson S. (1999) The geochemistry of redox sensitive trace metals in sediments. *Geochim. Cosmochim. Acta* **63**, 1735–1750.

Parrish R. R., Thirlwall M. F., Pickford C., Horstwood M., Gerdes A., Anderson J. and Coggon D. (2006) Determination of U-238/U-235, U-236/U-238 and uranium concentration in urine using SF-ICP-MS and MC-ICP-MS: an interlaboratory comparison. *Health Phys.* **90**(2), 127–138.

Püttmann W., Heppenheimer H. and Diedel R. (1990) Accumulation of copper in the Permian Kupferschiefer: a result of post-depositional redox reaction. *Org. Geochem.* **16**, 1145–1156.

Rademacher L. K., Lundstrom C. C., Johnson T. M., Sanford R. A., Zhao J. and Zhang Z. (2006) Experimentally determined uranium isotope fractionation during reduction of hexavalent U by bacteria and zero valent iron. *Environ. Sci. Technol.* **40**, 6943–6948.

Rehkämper M., Frank M., Hein J. R. and Halliday A. (2004) Cenozoic marine geochemistry of thallium deduced from isotopic studies of ferromanganese crusts and pelagic sediments. *Earth Planet. Sci. Lett.* **219**, 77–91.

Rehkämper M., Frank M., Hein J. R., Porcelli D., Halliday A., Ingri J. and Liebetrau V. (2002) Thallium isotope variations in seawater and hydrogenetic, diagenetic, and hydrothermal ferromanganese deposits. *Earth Planet. Sci. Lett.* **197**, 65–81.

Richter S., Alonso A., De Bolle W., Wellum R. and Taylor P. D. P. (1999) Isotopic "fingerprints" for natural uranium ore samples. *Int. J. Mass Spectrom.* **193**(1), 9–14.

Richter S. and Wellum R. (2006) Results for the "REINIEP 18" inter-laboratory comparison campaign for the measurement of uranium isotope ratios. *Geochim. Cosmochim. Acta* **70**(18), A532.

Robinson L. F., Belshaw N. S. and Henderson G. M. (2004) U and Th concentrations and isotope ratios in modern carbonates and waters from the Bahamas. *Geochim. Cosmochim. Acta* **68**(8), 1777–1789.

Rosman K. J. R. and Taylor P. D. P. (1998) Isotopic composition of the elements 1989. *Pure Appl. Chem.* **70**, 217–235.

Russel W. A., Papanastassiou D. A. and Tombrello T. A. (1978) Ca isotope fractionation on the Earth and other Solar System materials. *Geochim. Cosmochim. Acta* **42**, 1075–1090.

Schauble E. A. (2004) Applying stable isotope fractionation theory to new systems. In *Geochemistry of Non-traditional Stable Isotopes*, vol. 55 (eds. C. M. Johnsos, B. L. Beard and F. Albarede). pp. 65–111.

Schauble E. A. (2006) Equilibrium uranium isotope fractionation by nuclear volume and mass-dependent processes. *Fall Meeting*. V21B-0570 (abstr.).

Schauble E. A. (2007) Role of nuclear volume in driving equilibrium stable isotope fractionation of mercury, thallium, and other very heavy elements. *Geochim. Cosmochim. Acta* **71**, 2170–2189.

Schroeder E. and Stommel H. (1969) How representative is series of Panulirus stations of monthly mean conditions off Bermuda. *Prog. Oceanogr.* **5**, 31–40.

Siebert C., McManus J., Bice A., Poulson R. and Berelson W. M. (2006) Molybdenum isotope signatures in continental margin marine sediments. *Earth Planet. Sci. Lett.* **241**(3–4), 723–733.

Siebert C., Nägler T. F. and Kramers J. D. (2001) Determination of molybdenum isotope fractionation by double-spike multicollector inductively coupled plasma mass spectrometry. *Geochem. Geophys. Geosyst.* **2**. doi:10.1029/2000GC000124.

Siebert C., Nägler T. F., von Blanckenburg F. and Kramers J. D. (2003) Molybdenum isotope records as a potential new proxy for paleooceanography. *Earth Planet. Sci. Lett.* **211**, 159–171.

Stirling C. H., Andersen M. B., Potter E.-K. and Halliday A. N. (in press) Low-temperature isotopic fractionation of uranium. *Earth Planet. Sci. Lett.* **264**, 208–225.

Stirling C. H., Halliday A. N. and Porcelli D. (2005) In search of live 247Cm in the early solar system. *Geochim. Cosmochim. Acta* **69**, 1059–1071.

Suzuki Y. and Banfield J. F. (1999) Geomicrobiology of U. In *Uranium: Mineralogy, Geochemistry and the Environment*, vol. 38 (eds. P. C. Burns and R. Finch). pp. 393–431.

Tribovillard N., Algeo T., Lyons T. and Riboulleau A. (2006) Trace metals as paleoredox and paleoproductivity proxies: an update. *Chem. Geol.* **232**, 12–32.

Tyson R. V. and Pearson T. H. (1991) Modern and ancient continental shelf anoxia: an overview. In *Modern and Ancient Continental Shelf Anoxia*, vol. 58 (eds. R. V. Tyson and T. H. Pearson). Geololgical Society Special Publications, pp. 1–26.

Walder A. J. and Freedman P. A. (1992) Isotopic ratio measurement using a double focusing magnetic sector mass analyser with an inductively coupled plasma as an ion source. *J. Anal. At. Spectrom.* **7**, 571–575.

Wersin P., Hochella M. F., Persson P., Redden G., Leckie J. O. and Harris D. W. (1994) Interaction between aqueous uranium (VI) and sulfide minerals: spectroscopic evidence for sorption and reduction. *Geochim. Cosmochim. Acta* **58**, 2829–2843.

Weyer S., Anbar A. D., Brey G. P., Münker C., Mezger K. and Woodland A. B. (2005) Iron isotope fractionation during planetary differentiation. *Earth Planet. Sci. Lett.* **240**, 251–264.

Weyer S. and Schwieters J. B. (2003) High precision Fe isotope measurements with high mass resolution MC-ICPMS. *Int. J. Mass Spectrom.* **226**, 355–368.

Wombacher F., Rehkamper M., Mezger K. and Munker C. (2003) Stable isotope compositions of cadmium in geological materials and meteorites determined by multiple-collector ICPMS. *Geochim. Cosmochim. Acta* **67**, 4639–4654.

Zheng Y., Anderson R. F., Van Geen A. and Fleisher M. Q. (2002a) Remobilization of authigenic uranium in marine sediments by bioturbation. *Geochim. Cosmochim. Acta* **66**(10), 1759–1772.

Zheng Y., Anderson R. F., van Green a. and Fleischer M. Q. (2002b) Preservation of non-lithogenic particulate uranium in marine sediments. *Geochim. Cosmochim. Acta* **66**, 3085–3092.

Associate editor: James McManus